doi:10.1017/S143192761600845X
Microsc. Microanal. 22 (Suppl 3), 2016

Correlative Aberration-Corrected STEM-HAADF and STEM-EELS Analysis of Interface-Induced Polarization in $LaCrO_3$-$SrTiO_3$ Superlattices

Steven R. Spurgeon[1], Despoina M. Kepaptsoglou[2], Lewys Jones[3], Ryan B. Comes[1], Quentin M. Ramasse[2], Phuong-Vu Ong[1], Peter V. Sushko[1], and Scott A. Chambers[1]

[1.] Physical and Computational Sciences Directorate, Pacific Northwest National Laboratory, Richland, Washington, USA
[2.] SuperSTEM, SciTech Daresbury Campus, Daresbury, UK
[3.] Department of Materials, University of Oxford, Oxford, UK

Emergent phenomena at complex oxide interfaces continue to attract attention as the basis for a variety of next-generation devices, including photovoltaics and spintronics. Tremendous progress has been made toward understanding the role of interfacial defects, cation intermixing, and film stoichiometry in single heterojunction systems; however, the techniques commonly used to study these interfaces, such as X-ray photoelectron and absorption spectroscopies, are either sensitive only to near-surface regions or do not offer depth resolution to probe individual interfaces. Here we explore the induced polarization in superlattices of $LaCrO_3$ (LCO) and $SrTiO_3$ (STO) using a combination of aberration-corrected scanning transmission electron microscopy (STEM) and monochromated electron energy loss spectroscopy (STEM-EELS). We show that a correlative approach, utilizing an array of local and non-local probes, is necessary to fully understand the defect-mediated origin of the induced polarization in this system.

We have conducted detailed structural characterization of several LCO-STO superlattices, as shown in Figure 1. We employ high-angle annular dark field imaging (STEM-HAADF) to directly measure the induced ferroelectric polarization in the STO layers. We first acquire a relatively high-speed time series of multiple fast frames (0.4 μs px^{-1}), which are then aligned using both rigid and non-rigid registration to remove both sample drift and scan distortion [1]. Using this procedure we directly measure the induced ferroelectric polarization with picometer precision, as we have demonstrated elsewhere [2]. Our results reveal that the built-in asymmetric potential across the LCO / STO interfaces is sufficient to induce a sizable polarization, on the order of 40-70 μC cm^{-2}, in good agreement with *ab initio* calculations [3].

We next perform detailed characterization of chemical intermixing and local electronic fine structure changes to explore how defects affect the induced polarization. Figure 2 shows the result of monochromated EELS measurements of the Ti L_{23} edge fine structure, overlaid onto the integrated Ti L_{23} edge signal. An improved energy resolution of better than 0.120 eV allows us to observe significant Ti intermixing through the superlattice, as well as subtle fine structure changes in the vicinity of the LCO layers not apparent in earlier data. Mapping the Ti L_3 $t_{2g} - e_g$ crystal field splitting across the film, we find evidence consistent with a slight reduction in Ti valence from 4+ to 3+ in the vicinity of the LCO layers, possibly the consequence of La^{3+} substitution for Sr^{2+} or oxygen vacancies. Measurements of the Ti L_3 t_{2g} / e_g ratio also point toward such a trend: moving from the STO toward the LCO layers the ratio begins to decrease within the intermixed region, indicating a redistribution of electrons from t_{2g} to e_g states, suggesting a reduction in valence. In light of these results, our experimental STEM-HAADF measurements and accompanying *ab initio* calculations indicate that the induced polarization is robust against even sizable chemical intermixing and defect formation.

References:
[1] Jones, L. *et al*, "Smart Align – a new tool for robust non-rigid registration of scanning microscope data", *Advanced Structural & Chemical Imaging* **1**:8 (2015).
[2] Spurgeon, S. R. *et al,* "Polarization screening-induced magnetic phase gradients at complex oxide interfaces." *Nat. Commun.* 6, 1–11 (2015).
[3] Comes, R.B. *et al*, "Interface-induced Polarization in $SrTiO_3$-$LaCrO_3$ Superlattices." *Adv. Mater. Int.* In press (2016).

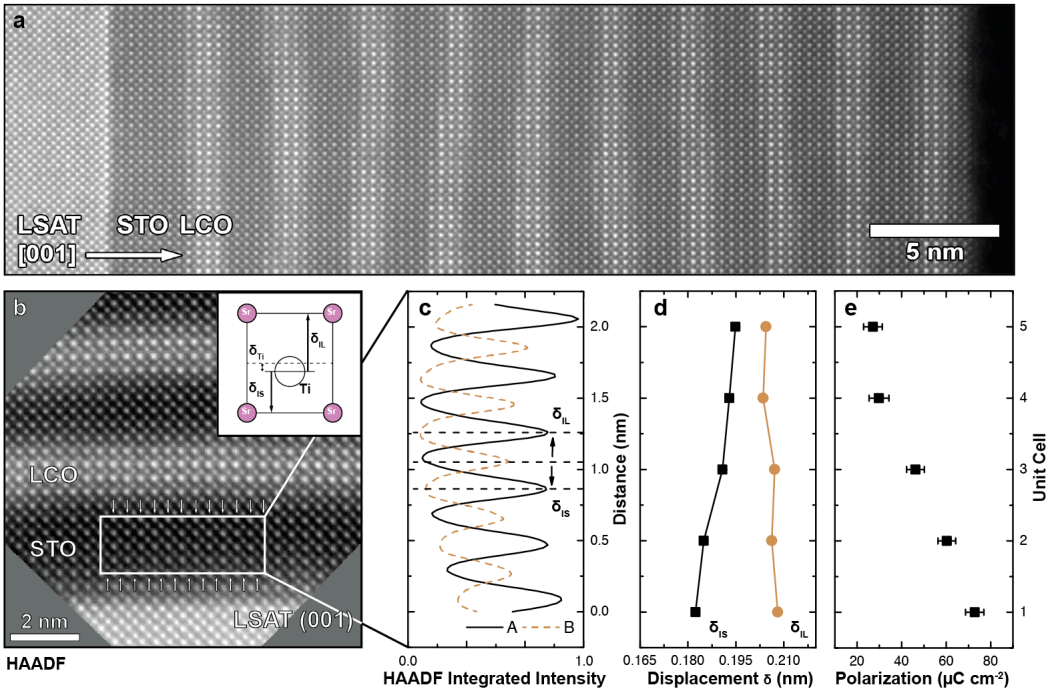

Figure 1: STEM analysis of induced polarization. A) Representative STEM-HAADF micrograph and model of the 6 u.c. $SrTiO_3$ - 3 u.c. $LaCrO_3$ superlattice with STO cap. B) Drift-corrected representative cross-sectional STEM-HAADF micrograph of the STO buffer layer, inset with an illustration of the unit cell. C) Average intensity profiles of the *A*- and *B*-site columns in A. D) Measurement of the short and long displacement vectors for each unit cell. E) Estimate of local polarization for each unit cell.

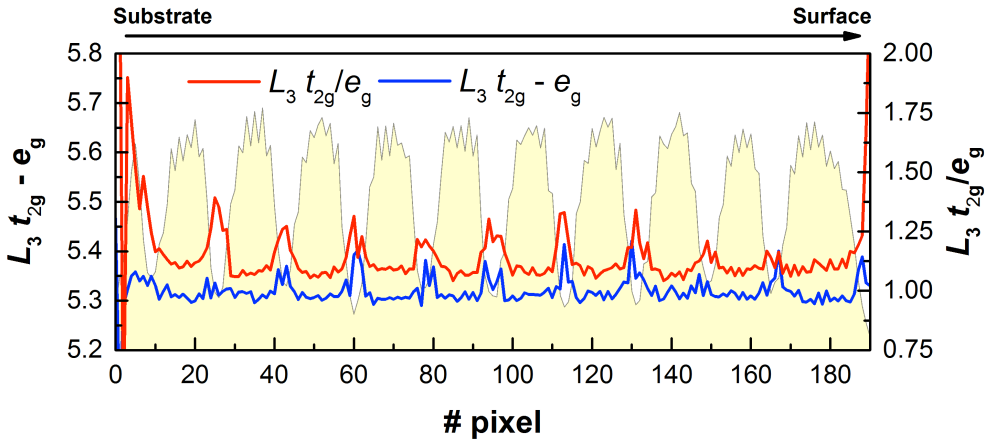

Figure 2: Monochromated EELS analysis. Measurement of Ti L_3 t_{2g} / e_g peak ratio and L_3 t_{2g} - e_g crystal field splitting parallel to the superlattice growth direction, overlaid with integrated Ti L_{23} signal.

https://doi.org/10.1017/S143192761600845X Published online by Cambridge University Press